

## Supporting Information

### Simultaneous Reduction of Surface, Bulk, and Interface Recombination for Au Nanoparticles Embedded Hematite Nanorod Photoanodes toward Efficient Water Splitting

Lei Wang,<sup>a,b,\*</sup> Tomohiko Nakajima,<sup>c</sup> Yan Zhang<sup>d</sup>

a. College of Chemistry and Chemical Engineering and Inner Mongolia Key Lab of Nanoscience and Nanotechnology, Inner Mongolia University, , Hohhot, 010021 P. R. China.

E-mail: [wanglei@imu.edu.cn](mailto:wanglei@imu.edu.cn)

b. State Key Laboratory for Oxo Synthesis and Selective Oxidation, National Engineering Research Center for Fine Petrochemical Intermediates, Lanzhou Institute of Chemical Physics, Chinese Academy of Sciences, Lanzhou 730000, China.

c. Advanced Coating Technology Research Center, National Institute of Advanced Industrial Science and Technology, Tsukuba Central 5, 1-1-1 Higashi, Tsukuba, Ibaraki 305-8565, Japan.

d. College of Physics and Electronic Engineering, Northwest Normal University, Lanzhou 730000, China.

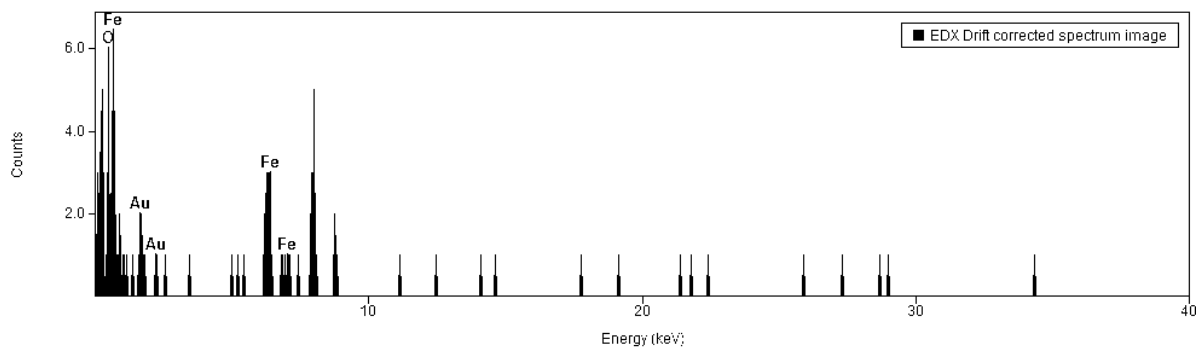


**Figure S1.** EDX scanning of Au/Fe<sub>2</sub>O<sub>3</sub> NRs.

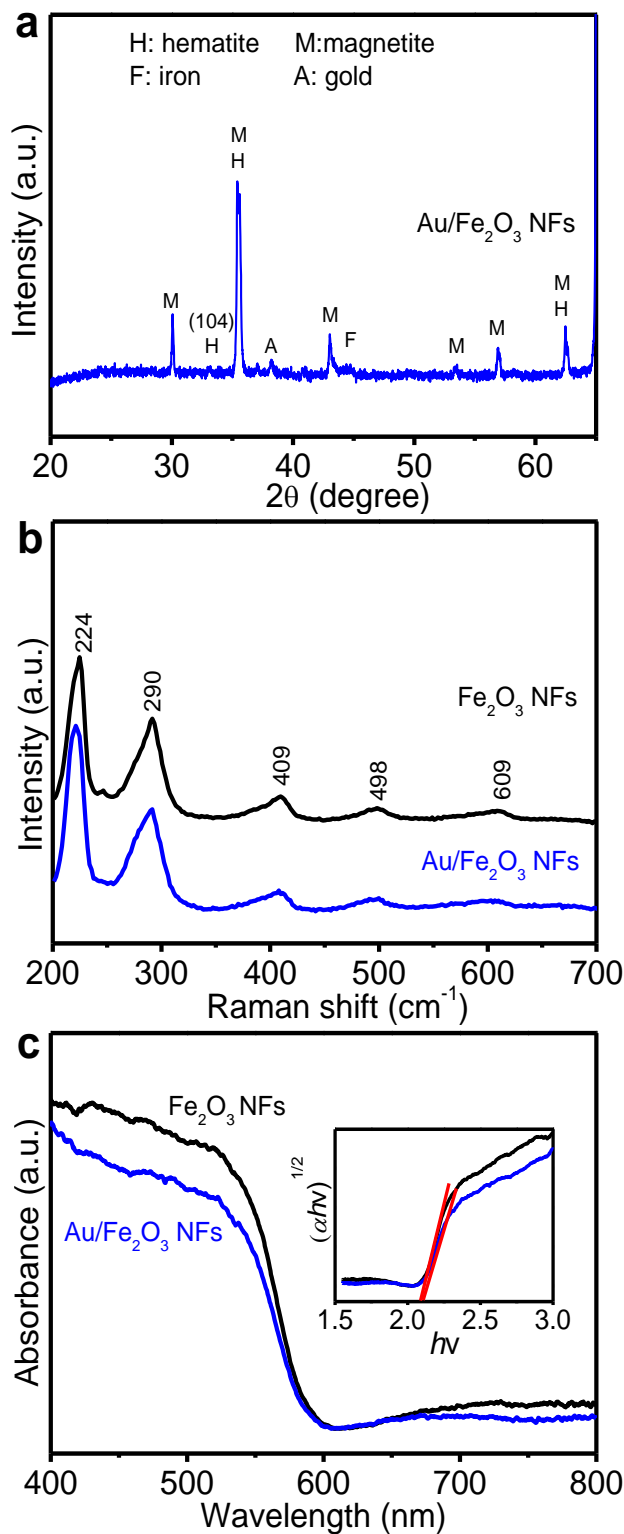


**Figure S2.** (a) XRD pattern, (b) Raman spectrum, and (c) UV-vis diffuse reflectance spectrum of  $\text{Au}/\text{Fe}_2\text{O}_3$  NFs. The results of  $\text{Fe}_2\text{O}_3$  NFs were shown for comparison. H:  $\text{Fe}_2\text{O}_3$ ; M:  $\text{Fe}_3\text{O}_4$ ; F: Fe; A: Au.

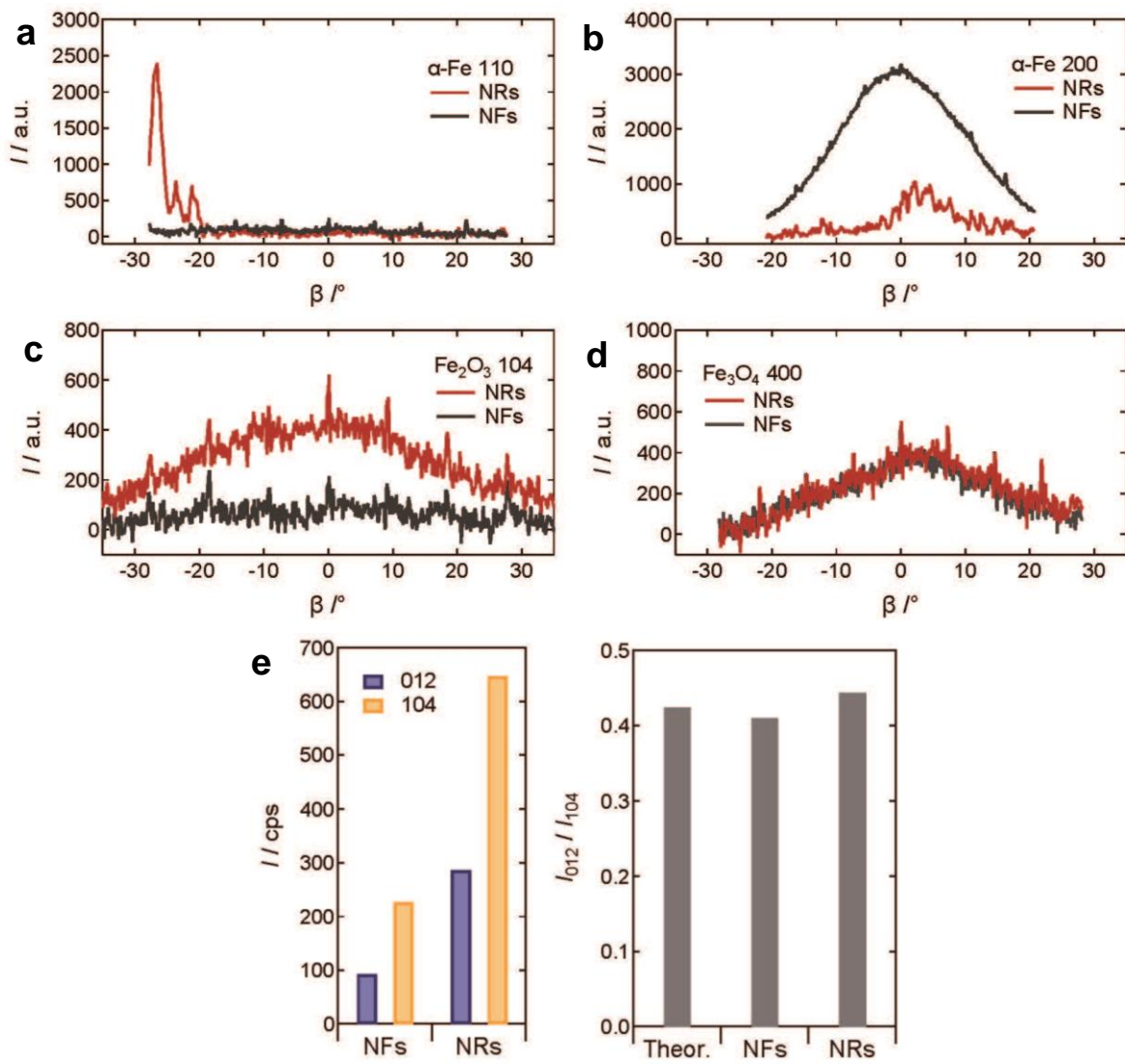


**Figure S3.** Comparison of 2D XRD patterns of  $\text{Fe}_2\text{O}_3$  NFs (NFs) and Au/ $\text{Fe}_2\text{O}_3$  NRs (NRs).

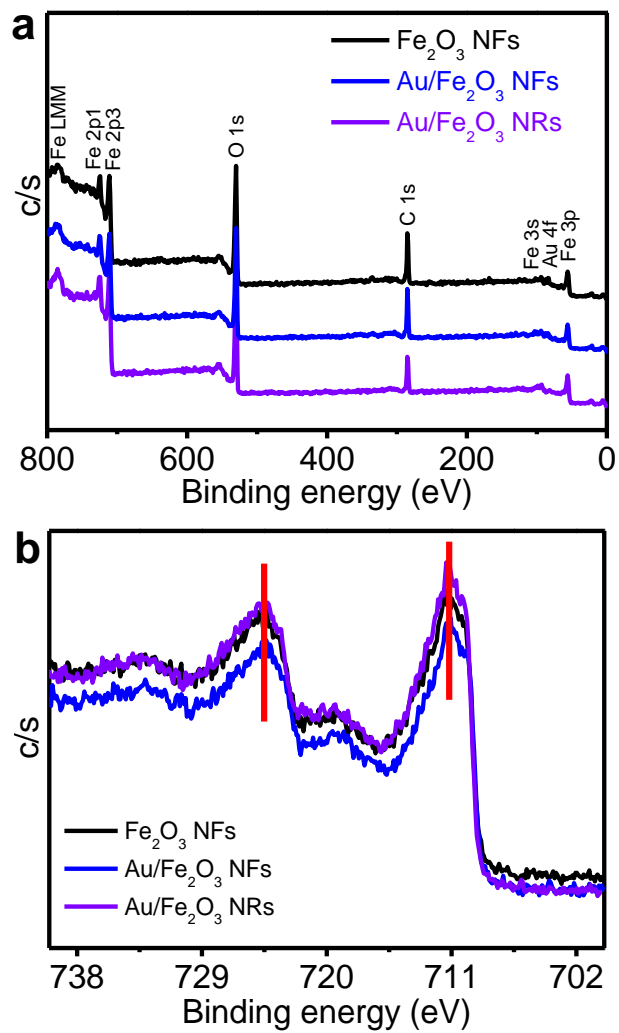


**Figure S4.** (a) XPS survey spectra, and (b) high resolution Fe 2p of  $\text{Fe}_2\text{O}_3$  NFs,  $\text{Au}/\text{Fe}_2\text{O}_3$  NFs, and  $\text{Au}/\text{Fe}_2\text{O}_3$  NRs.

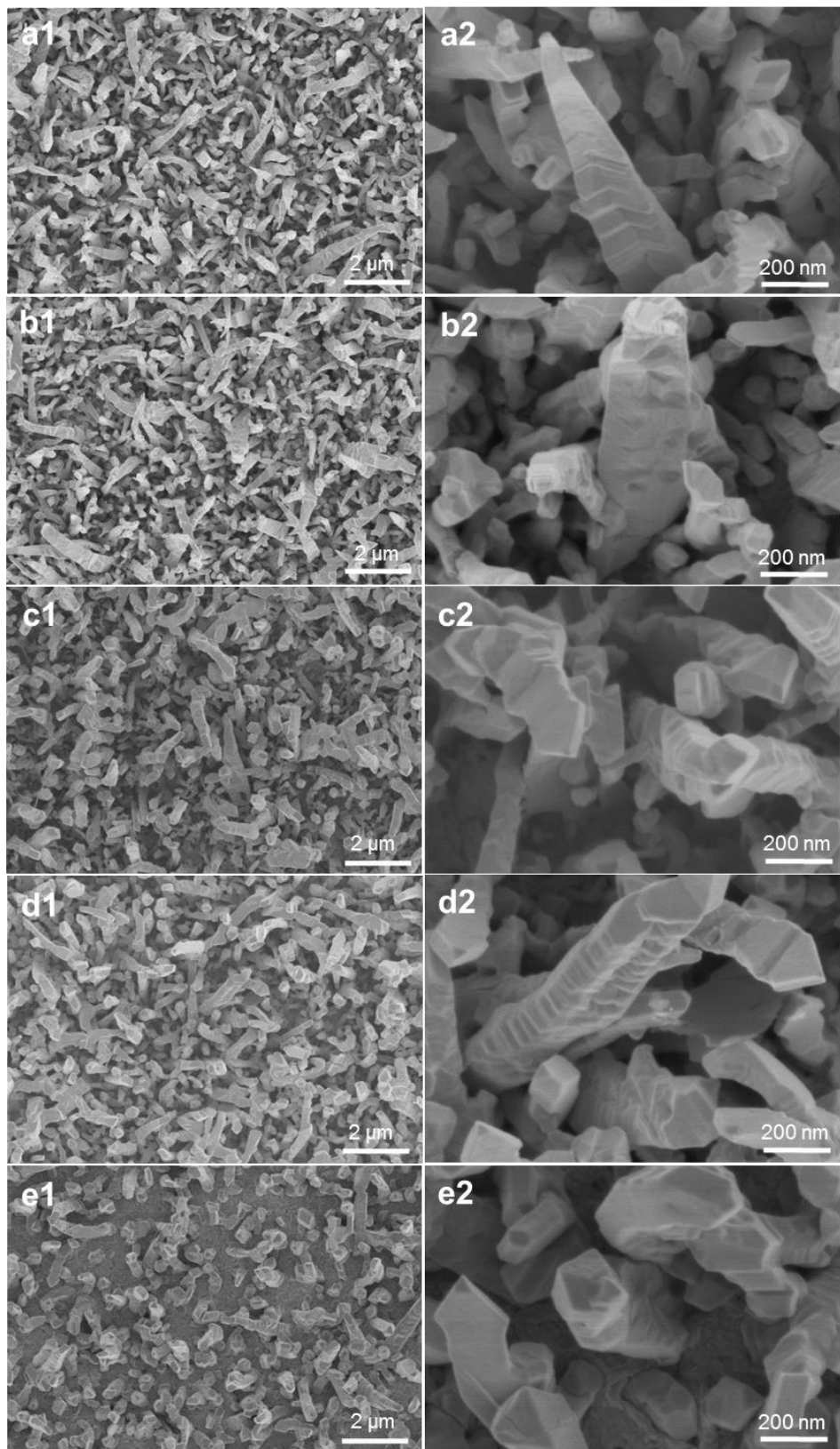


**Figure S5.** SEM images of Au/Fe<sub>2</sub>O<sub>3</sub> NRs. The Au/Fe<sub>2</sub>O<sub>3</sub> NFs were annealed in Ar atmosphere at various temperatures. (a) 500 °C; (b) 550 °C; (c) 600 °C; (d) 650 °C; (e) 700 °C.

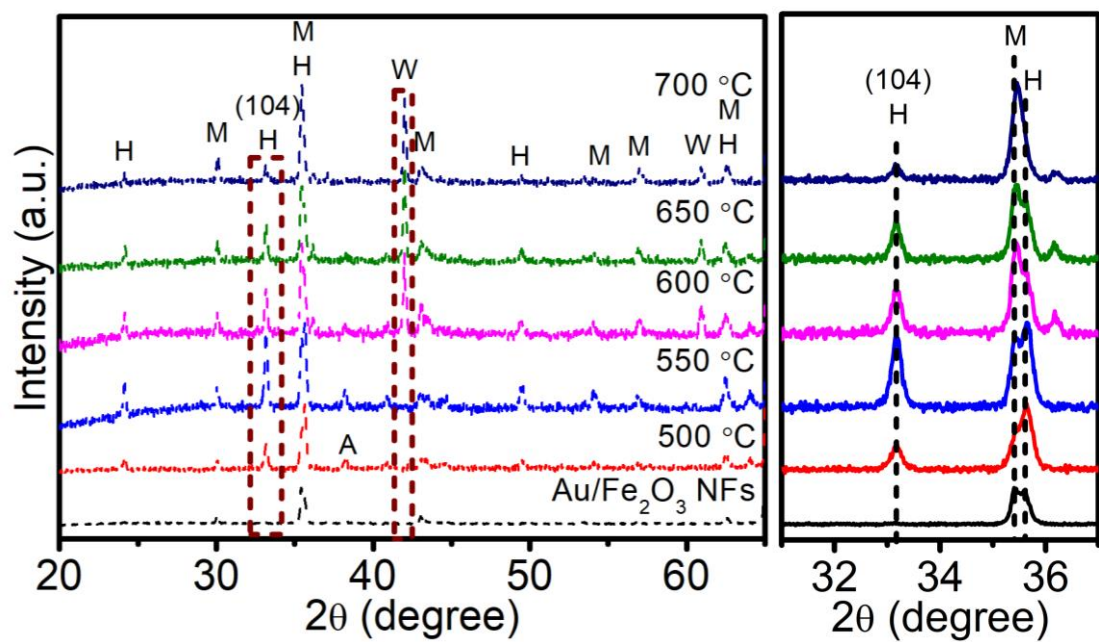


**Figure S6.** XRD patterns of Au/Fe<sub>2</sub>O<sub>3</sub> NRs annealing in Ar atmosphere at various temperatures. H: Fe<sub>2</sub>O<sub>3</sub>; M: Fe<sub>3</sub>O<sub>4</sub>; W: FeO; A: Au.

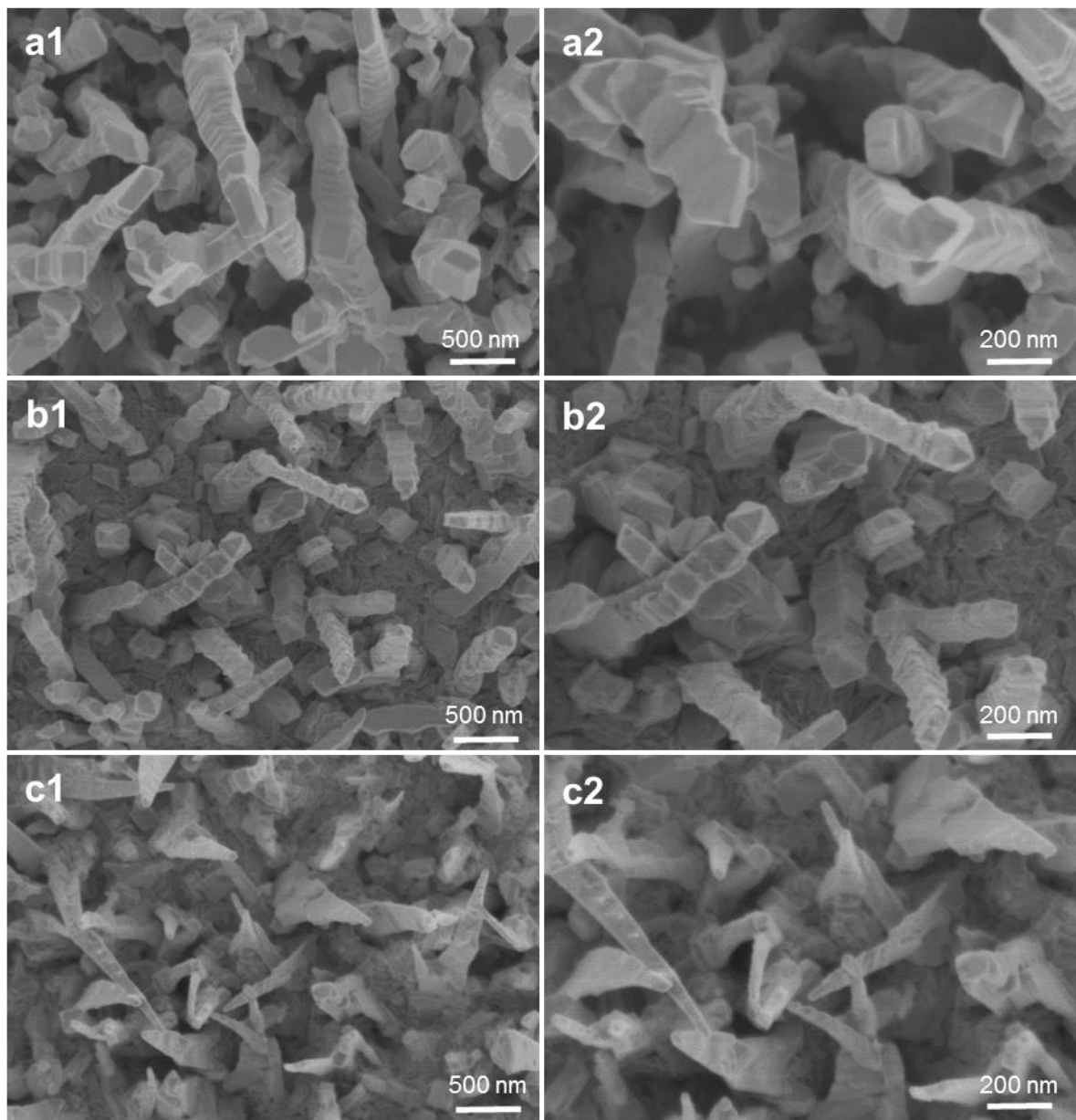


**Figure S7.** SEM images of (a) Au/Fe<sub>2</sub>O<sub>3</sub> NRs, (b) Ti/Fe<sub>2</sub>O<sub>3</sub> NRs, and (c) P/Fe<sub>2</sub>O<sub>3</sub> NRs.

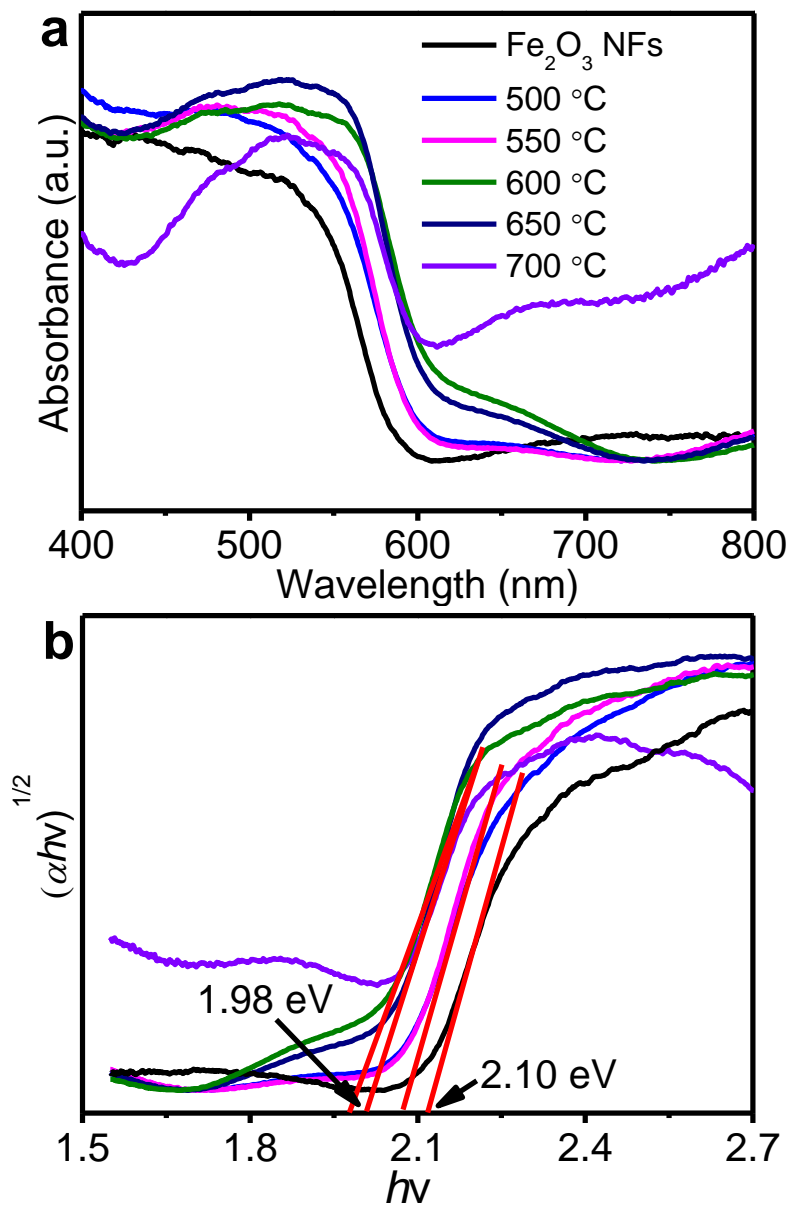


**Figure S8.** (a) UV-vis diffuse reflectance spectra and (b) calculation of band gaps of  $\text{Au}/\text{Fe}_2\text{O}_3$  NRs. The  $\text{Au}/\text{Fe}_2\text{O}_3$  NFs were annealed in Ar atmosphere at various temperatures.

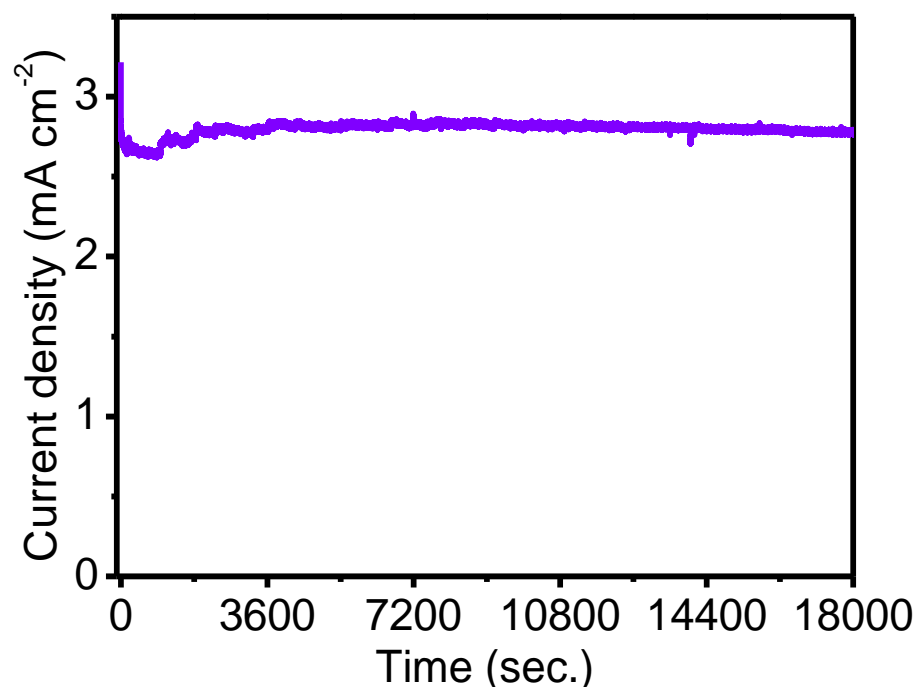


**Figure S9.** Stability of Au/Fe<sub>2</sub>O<sub>3</sub> NRs applied at 1.5 V<sub>RHE</sub>.

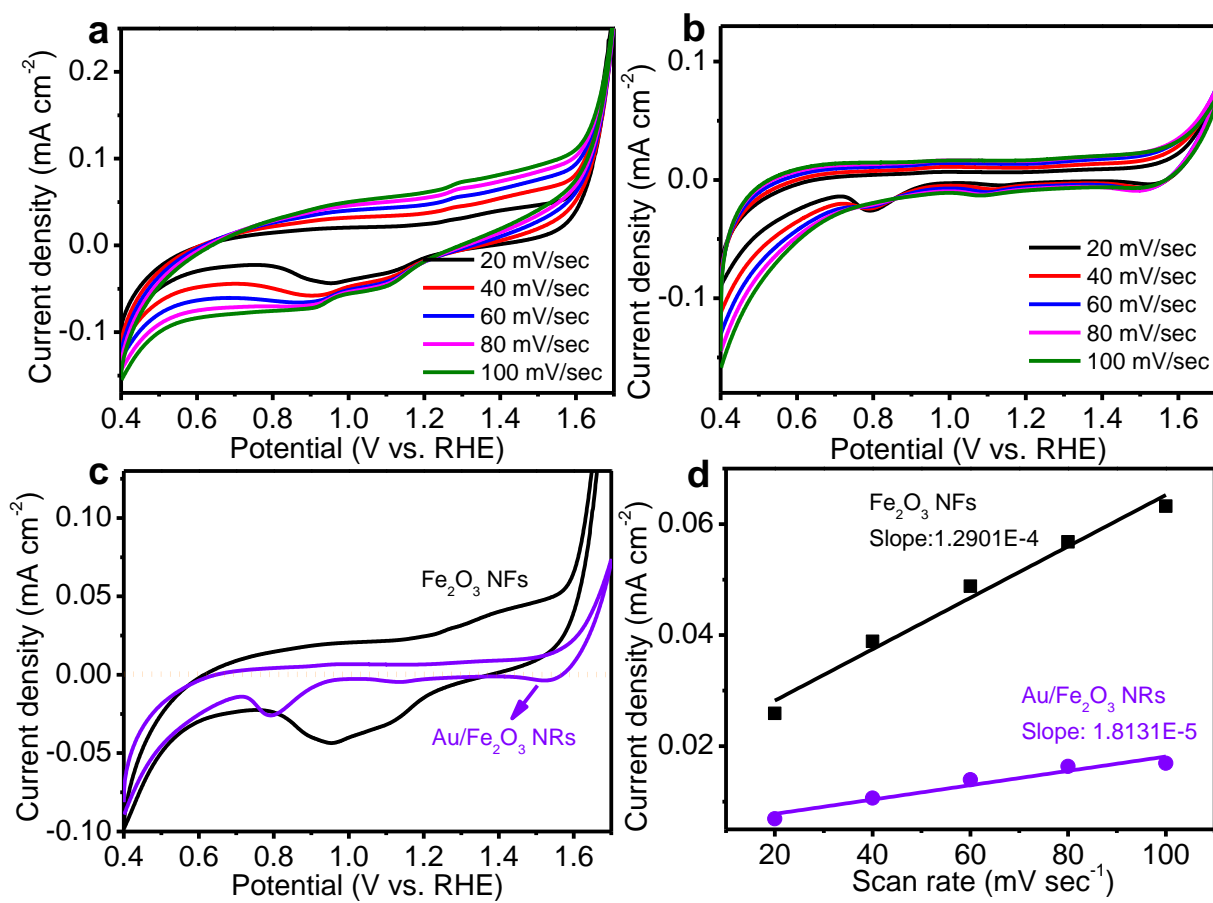


**Figure S10.** (a-c) Cyclic voltammetry curves and (d) relative electrochemical surface areas of  $\text{Fe}_2\text{O}_3$  NFs and  $\text{Au}/\text{Fe}_2\text{O}_3$  NRs.

As scan rate increases from 20 to 100  $\text{mV sec}^{-1}$ , the current increases while a small positive shift of the oxidation peak potential and a negative shift of the reduction peak potential have been observed with the increased scan rate. It should be related to the reaction capability and the  $\text{OH}^-$  concentration at the interface between the electrode and electrolyte.

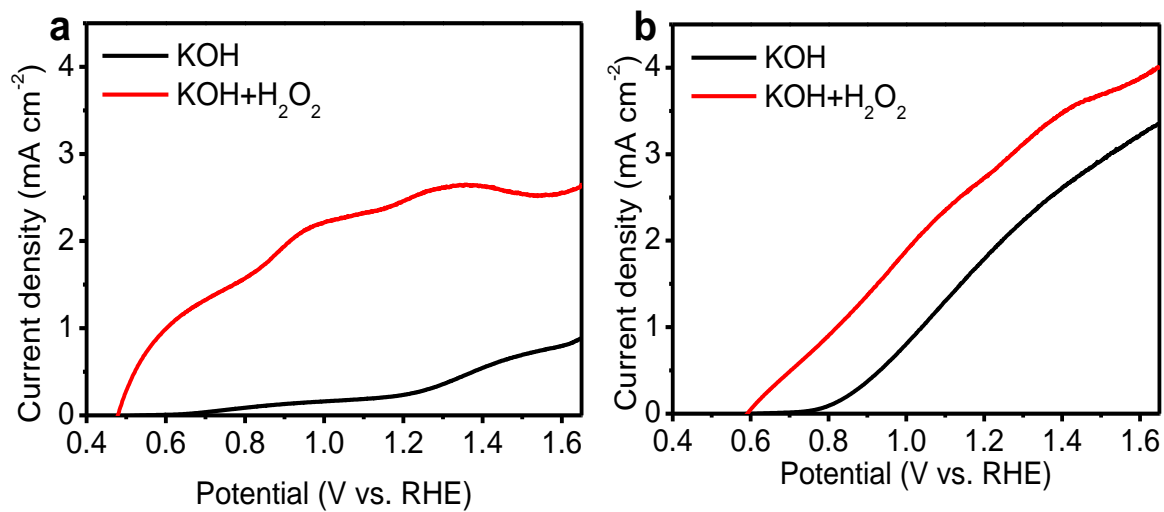


**Figure S11.** Linear sweep voltammogram (LSV) curves of (a)  $\text{Fe}_2\text{O}_3$  NFs and (b)  $\text{Au}/\text{Fe}_2\text{O}_3$  NRs in 1 M KOH electrolytes without and with  $\text{H}_2\text{O}_2$ .

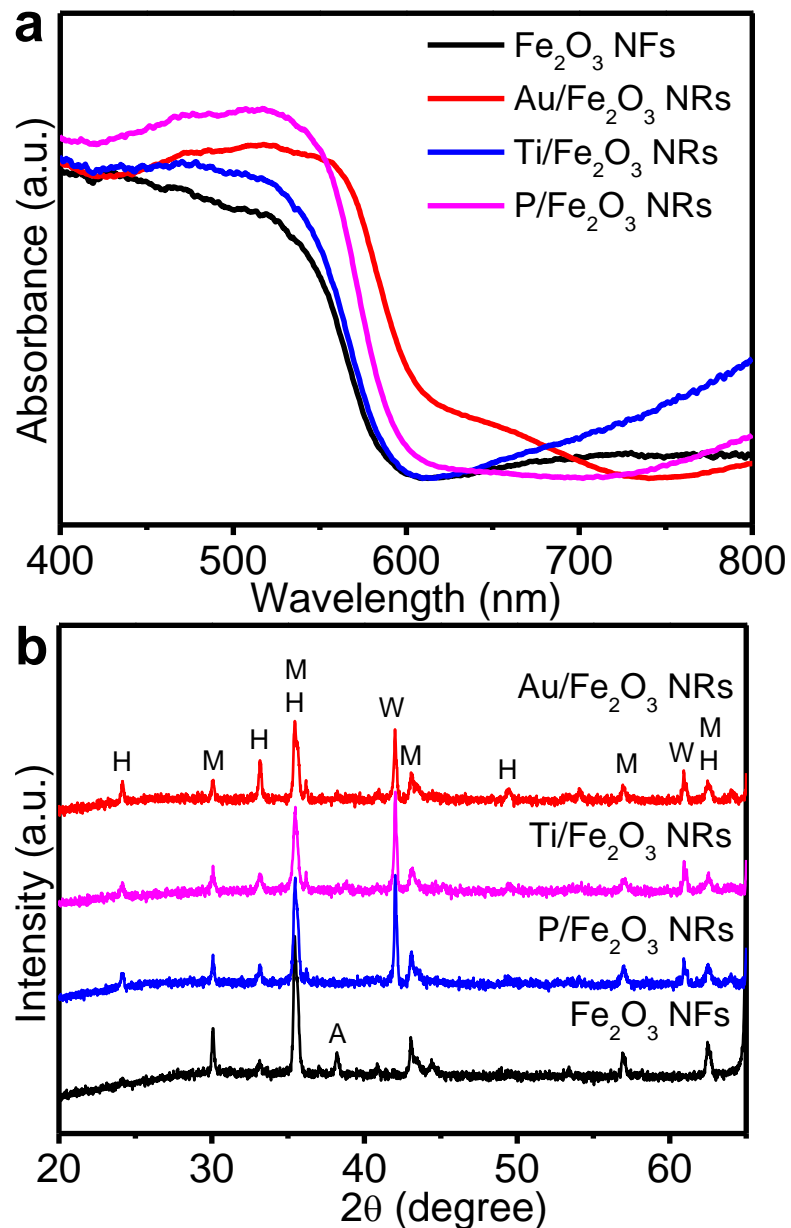


**Figure S12.** (a) UV-vis diffuse reflectance spectra, and (b) XRD patterns of  $\text{Au}/\text{Fe}_2\text{O}_3$  NRs,  $\text{Ti}/\text{Fe}_2\text{O}_3$  NRs, and  $\text{P}/\text{Fe}_2\text{O}_3$  NRs. H:  $\text{Fe}_2\text{O}_3$ ; M:  $\text{Fe}_3\text{O}_4$ ; W:  $\text{FeO}$ ; F: Fe; A: Au.

**Table S1** Comparison of photoresponses of recent hematite electrodes in solar water splitting under AM 1.5G illumination.<sup>1-6</sup>

Photoanodes	$i @ 1.23 V_{RHE}$	Onset potential	Electrolyte
ITO/Fe <sub>2</sub> O <sub>3</sub> nanowires/Fe <sub>2</sub> TiO <sub>5</sub> /FeNiOOH on FTO <sup>1</sup>	2.2 mA cm <sup>-2</sup>	~0.95 V <sub>RHE</sub>	1 M NaOH
Gradient P doped Fe <sub>2</sub> O <sub>3</sub> nanobundles on FTO <sup>2</sup>	~1.48 mA cm <sup>-2</sup>	0.8 V <sub>RHE</sub>	1 M KOH
CoFeO <sub>x</sub> /Fe <sub>2</sub> O <sub>3</sub> NRs on FTO <sup>3</sup>	1.2 mA cm <sup>-2</sup>	~0.6 V <sub>RHE</sub>	1 M NaOH
Zr induced Fe <sub>2</sub> O <sub>3</sub> nanotubes on FTO <sup>4</sup>	1.5 mA cm <sup>-2</sup>	~0.85 V <sub>RHE</sub>	1 M NaOH
Ti doped Fe <sub>2</sub> O <sub>3</sub> NRs on FTO <sup>5</sup>	2.5 mA cm <sup>-2</sup>	~0.85 V <sub>RHE</sub>	1 M KOH
Ti doped Fe <sub>2</sub> O <sub>3</sub> NRs on FTO <sup>6</sup>	2.4 mA cm <sup>-2</sup>	~0.95 V <sub>RHE</sub>	1 M NaOH
<b>Au/Fe<sub>2</sub>O<sub>3</sub> on Fe substrate in this work</b>	<b>2.0 mA cm<sup>-2</sup></b>	<b>0.6 V<sub>RHE</sub></b>	1 M KOH

Table S1 compared the photocurrent densities for the hematite nanostructures in more recent years. Compared to the hematite nanostructures grown on FTO substrates, the Au/Fe<sub>2</sub>O<sub>3</sub> nanorods on iron substrate shows a relatively higher photoresponse, especially for a lower onset potential. A higher temperature annealing (700-800 °C) is introduced to activate the Fe<sub>2</sub>O<sub>3</sub> on FTO substrates, and Sn doping in the Fe<sub>2</sub>O<sub>3</sub> nanostructures.

## References

- P. Tang, H. Xie, C. Ros, L. Han, M. Biset-Peiró, Y. He, W. Kramer, A. P. Rodríguez, E. Saucedo, J. R. Galán-Mascarós, T. Andreu, J. R. Morante and J. Arbiol, *Energy Environ. Sci.*, 2017, **10**, 2124.
- Z. Luo, C. Li, S. Liu, T. Wang and J. L. Gong, *Chem. Sci.*, 2017, **8**, 91.
- J. Zhang, R. García-Rodríguez, P. Cameron and S. Eslava, *Energy Environ. Sci.*, 2018, **11**, 2972.
- C. Li, A. Li, Z. Luo, J. Zhang, X. Chang, Z. Huang, T. Wang and J. L. Gong, *Angew. Chem. Int. Ed.*, 2017, **129**, 4214.
- Z. Luo, T. Wang, J. Zhang, C. Li, H. Li and J. L. Gong, *Angew. Chem. Int. Ed.*, 2017, **56**, 12878.
- Z. Wang, X. Mao, P. Chen, M. Xiao, S. A. Monny, S. Wang, M. Konarova, A. Du and L. Wang, *Angew. Chem. Int. Ed.*, 2018, **131**, 1042.